J|A|C|S ARTICLES

Published on Web 06/03/2009

Distinct Role of Specific Tryptophans in Facilitating Electron Transfer or as [Fe(IV)=O Trp$^{\bullet}$] Intermediates in the Peroxidase Reaction of *Bulkholderia pseudomallei* Catalase-Peroxidase: A Multifrequency EPR Spectroscopy Investigation

Julie Colin,[‡] Ben Wiseman,[§] Jacek Switala,[§] Peter C. Loewen,[§] and Anabella Ivancich*[,‡]

CNRS URA 2096, CEA, IBITEC, F-91191 Gif-sur-Yvette, France, and Department of Microbiology, University of Manitoba, Winnipeg, Canada R3T 2N2

Received February 24, 2009; E-mail: anabella.ivancich@cea.fr

Abstract: We have characterized the reactive intermediates of the peroxidase-like reaction of *Bulkholderia pseudomallei* KatG using multifrequency EPR spectroscopy. The aim was to investigate the putative role of tryptophanyl radicals as alternative intermediates to the [Fe(IV)=O Por$^{\bullet+}$] species or as short-lived species involved in superexchange-coupled pathways between redox cofactors. Three distinct sites for the formation of radical intermediates, Trp330, Trp139 and Trp153, were identified using single, double and triple variants of *Bulkholderia pseudomallei* KatG. The proximal Trp330 is the site for a radical in magnetic interaction with the ferryl heme iron [Fe(IV)=O Trp$^{\bullet+}$], formed at the expense of a short-lived [Fe(IV)=O Por$^{\bullet+}$] species as in the cases of *Mycobacterium tuberculosis* KatG and cytochrome c peroxidase. Formation of the Trp153 radical at a site close to the enzyme surface crucially depends on the integrity of the H-bonding network of the heme distal side, that includes Trp95, the radical site in the *Synechocystis* KatG. Accordingly, the extended H-bonding network and Trp94 provide an electron transfer pathway between Trp153 and the heme. The distal tryptophan (Trp111) being part of the KatG-specific adduct required for the catalase-like activity, is involved in facilitating electron transfer for the formation of the Trp139 radical. We propose a comprehensive description of the role of specific Trp residues that takes into account not only the apparent differences in sites for the Trp$^{\bullet}$ intermediates in other catalase-peroxidases but also the similar cases observed in monofunctional peroxidases.

Introduction

Catalase-peroxidases (KatGs) are heme-containing enzymes encoded by the *katG* gene in different bacteria named after their capability to perform efficiently the two-electron oxidation and reduction reactions with two molecules of hydrogen peroxide per cycle (catalase-like reaction). These enzymes are also efficient in the one-electron oxidation of substrate(s) by means of a higher valence intermediate (peroxidase-like reaction). The specific interest in catalase-peroxidases, and in particular in the *Mycobacterium tuberculosis* KatG (MtKatG) was triggered by the evidence associating the deletion of the *katG* gene from *M. tuberculosis* chromosome with the resistance to treatment with the front-line prodrug isoniazid (isonicotinic acid hydrazide, INH) in clinical isolates.[1] A more general interest in the study of KatGs, which are phylogenetically related to monofunctional peroxidases[2,3] arises from the unrivalled possibility to directly investigate the structural and/or functional features allowing dual enzymatic reactions in a single enzyme.

The high-resolution crystallographic structures of resting and oxidized *Bulkholderia pseudomallei* catalase-peroxidase (BpKatG) at different pH values[4−6] combined with activity and kinetic measurements provide a better understanding of the unique features conveying catalase-like activity to this enzyme. BpKatG presents few of the structural characteristics previously identified as a requirement in monofunctional catalases to efficiently disproportionate hydrogen peroxide. For example, the constricted and hydrophobic access channel and the π-stacking interaction of the distal His with the heme observed in monofunctional catalases[7,8] are absent in BpKatG. Yet, the KatG enzymes can efficiently perform the catalase-like reaction. Even more puzzling is the fact that the bifunctional KatGs and

[‡] CNRS URA 2096 and CEA-Saclay.
[§] University of Manitoba.

(1) Zhang, Y.; Heym, B.; Allen, B.; Young, D.; Cole, S. *Nature* **1992**, *358*, 591–593.
(2) Wellinder, K. *Biochim. Biophys. Acta* **1991**, *1080*, 215–220.
(3) (a) Klotz, M. G.; Loewen, P. C. *Mol. Biol. Evol.* **2003**, *20*, 1098–1112. (b) Passardi, F.; Zamocky, M.; Favet, J.; Jakopitsch, C.; Penel, C.; Obinger, C.; Dunand, C. *Gene* **2007**, *397*, 101–113.
(4) Carpena, X.; Loprasert, S.; Mongkolsuk, S.; Switala, J.; Loewen, P. C.; Fita, I. *J. Mol. Biol.* **2003**, *327*, 475–489.
(5) Carpena, X.; Wiseman, B.; Deemagarn, T.; Herguedas, B.; Ivancich, A.; Singh, R.; Loewen, P. C.; Fita, I. *Biochemistry* **2006**, *45*, 5171–5179.
(6) Deemagarn, T.; Wiseman, B.; Carpena, X.; Ivancich, A.; Fita, I.; Loewen, P. C. *Proteins* **2007**, *66*, 219–228.
(7) Mate, M. J.; Murshudov, G.; Bravo, J.; Melik-Adamyan, W.; Loewen, P. C.; Fita, I. In *Handbook of Metalloproteins*; J. Wiley & Sons: New York, NY, 2001; pp 486−502.

peroxidases show relatively high structural homology, but peroxidases have only residual catalase-like activity (for a review, see ref 9). Accordingly, we refer to the latter as monofunctional peroxidases.

In this work, we have focused on the characterization of the intermediates of the peroxidase-like reaction of BpKatG using multifrequency EPR spectroscopy. The aim was to understand better the putative role of specific tryptophan residues as alternative radical intermediates to the [Fe(IV)=O Por$^{\bullet+}$] species or as short-lived species in superexchange-coupled pathways between redox cofactors.[10,11] The content of tryptophans in catalase-peroxidases is remarkably high as compared to monofunctional peroxidases. It ranges from 22 to 25 in KatGs, while monofunctional peroxidases have a maximum number of 7 (in cytochrome *c* peroxidase). Our previous characterizations of the *Synechocystis*[12] (SynKatG) and *M. tuberculosis*[13] catalase-peroxidases showed differences in the sites for formation of Trp$^{\bullet}$ intermediates. This result is not surprising, considering the observed behavior of the monofunctional enzymes such as cytochrome c peroxidase[14] and lignin peroxidase.[15] In SynKatG, Trp106 was identified as the unique site for the [Fe(IV)=O Trp$^{\bullet}$] species formed subsequently to the [Fe(IV)=O Por$^{\bullet+}$] intermediate, despite the existence of 21 other tryptophans.[12] Trp106 is part of a short stretch of 11 residues, nonexistent in monofunctional peroxidases, and spanning the proximal and distal sides of the heme. The presence of these extra residues makes the heme cofactor in KatGs less surface exposed than in monofunctional peroxidases. It also delineates an extended H-bonding network on the heme distal side that includes Trp106 and which is required for the catalase-like activity of SynKatG.[16] In MtKatG, two Trp radicals were identified[13] as intermediates formed subsequently to a short-lived [Fe(IV)=O Por$^{\bullet+}$] intermediate. Yet, these Trp radical sites differed from that of SynKatG. Our findings on BpKatG demonstrate that the differences in radical sites in KatGs can be explained by variability in stabilization of the tryptophanyl radicals as reactive intermediates in this family of enzymes. Three distinct sites for the formation of radical intermediates, Trp330, Trp139, and Trp153, were identified in BpKatG using single, double, and triple Trp variants and EPR spectroscopy. The proximal Trp330 is the site for a radical in magnetic interaction with the ferryl heme iron, [Fe(IV)=O Trp$^{\bullet+}$] as in the case of MtKatG. The formation of the Trp153 radical at a site close to the enzyme surface crucially depends on the integrity of the distal-side extended H-bonding network[16] since the most probable electron transport pathway includes Trp94 and Trp95. Triple variants allowed us to demonstrate that the removal of Trp330, Trp139, and Trp153, the three sites for the stable radical intermediates of BpKatG, induces the formation of a longer-lived radical on Trp95 (the radical site in SynKatG). The characterization of the peroxidase reaction in BpKatG allowed us to elaborate a more complete picture of the role of specific Trp residues that accounts for the apparent differences in Trp$^{\bullet}$ intermediates among catalase-peroxidases, also including the few cases in monofunctional peroxidases for which tryptophans are also alternative intermediates to the [Fe(IV)=O Por$^{\bullet+}$] species.

Materials and Methods

Samples Preparation. Strains and Plasmids. The plasmid pBG306[17] was used as a source for catalase-peroxidase from *B. pseudomallei*. A 3369 bp *Kpn*I−*Eco*RI fragment was cloned into pKS- to generate pBpKatG, and an additional *Hin*dIII site was introduced at bp 1731 using the primer TGGTTC**AAGCTT**ACG-CAC to generate pBpKatG-H. A 1002 bp *Kpn*I−*Cla*I fragment was cloned from pBpKatG-H into KS+ to generate pBpG-KC (for mutagenesis of amino acids 1 to 180) and a 729 bp *Cla*I−*Hin*dIII fragment was cloned into pKS+ to generate pBpG-CH (for mutagenesis of amino acids 181 to 420). Plasmids were transformed into the catalase-deficient strain UM262 *pro leu rpsL hsdM hsdR endI lacY katG2 katE12*::Tn*10 recA*[18] for expression and isolation of the wild type and variant KatG proteins. Phagemids pKS^{+} and pKS^{-} from Stratagene Cloning Systems were used for mutagenesis, sequencing, and cloning. *E. coli* strains NM522 (*supE thi*)(*lac-proAB*) *hsd-5* [F′ *proAB lacI*^{q} *lacZ*)*15*][18] a, JM109 (*recA1 supE44 endA1 hsdR17 gyrA96 relA1 thi*) (*lac-proAB*),[19] and CJ236 (*dut-1 ung-1 thi-1 relA1*/pCJ105 F′)[20] were used as hosts for the plasmids and for generation of single-stranded phage DNA using helper phage R408.

Mutagenesis. The oligonucleotides TCGCATTAC**TTC**TGGC-CGGCC (TTC encoding Phe in place of Trp94), CAGGACTG-G**TTC**CCGGCCGAT (TTC encoding Phe in place of Trp95), CTCAACAGC**TTC**CCCGACAAC (TTC encoding Phe in place of Trp 139), CGGCTGCTG**TTC**CCGATCAAG (TTC encoding Phe in place of Trp 153), and GAAGTCACGTTCACGACGACG (TTC encoding Phe in place of Trp330) were purchased from Invitrogen. They were used to mutagenize either the 1002 bp fragment in pBpG-KC (for W94F, W95F, W139F and W153F) or the 729 bp fragment in pBpG-CH (for W330F) following the Kunkel procedure,[20] which were subsequently reincorporated into pBpKatG-H to generate the mutagenized *katG* genes. Double and triple variants were constructed either by ligation of individual mutagenized sequences or by mutagenization of previous variants as appropriate. Sequence confirmation of all sequences was done by the Sanger method[21] on double-stranded plasmid DNA generated in JM109. The plasmids were transformed into UM262 and grown in Luria broth containing 10 g/L tryptone, 5 g/L yeast extract, and 5 g/L NaCl for expression of the KatG. Subsequent purification of the enzymes was as described.[17] For better incorporation of heme, hemin chloride (40 mg·L^{-1}) was exogenously added to the growth medium.

Isotope Labeling. UM262 transformed with pBpKatG-H was grown in minimal medium for incorporation of perdeuterated tryptophan or perdeuterated tyrosine (CDN Isotopes). Isolation and purification of the deuterated enzymes was carried out as described previously for the nondeuterated samples.

(8) Loewen, P. C.; Carpena, X.; Perez-Luque, R.; Rovira, C.; Ivancich, A.; Haas, R.; Odenbreit, S.; Nicholls, P.; Fita, I. *Biochemistry* **2004**, *43*, 3089–3103.
(9) Dunford, B. H. *Heme Peroxidases* John Wiley & Sons, Inc.: New York, 1999.
(10) Page, C. C.; Moser, C.; Chen, X.; Dutton, L. *Nature* **1999**, *402*, 47–52.
(11) Shih, C.; Museth, A. K.; Abrahamsson, M.; Blanco-Rodriguez, A. M.; Di Biblio, A.; Sudhamsu, J.; Crane, B. R.; Ronayne, B. R.; Towrie, M.; Vlcek, A., Jr.; Richards, J. H.; Winkler, J. R.; Gray, H. B. *Science* **2008**, *320*, 1760–1762.
(12) Ivancich, A.; Jakopitsch, C.; Auer, M.; Un, S.; Obinger, C. *J. Am. Chem. Soc.* **2003**, *125*, 14093–14102.
(13) Singh, R.; Switala, J.; Loewen, P. C.; Ivancich, A. *J. Am. Chem. Soc.* **2007**, *129*, 15954–15963.
(14) Sivaraja, M.; Goodin, D. B.; Smith, M.; Hoffman, B. M. *Science* **1989**, *245*, 738–740.
(15) Doyle, W. A.; Blodig, W.; Veitch, N. C.; Piontek, K.; Smith, A. T. *Biochemistry* **1998**, *37*, 15097–15105.
(16) Jakopitsch, C.; Obinger, C.; Un, S.; Ivancich, A. *J. Inorg. Biochem.* **2006**, *100*, 1091–1099.
(17) Carpena, X.; Switala, J.; Loprasert, S.; Mongkolsuk, S.; Fita, I.; Loewen, P. C. *Acta Crystallogr.* **2002**, *D58*, 2184–2186.
(18) Triggs-Raine, B. L.; Loewen, P. C. *Gene* **1987**, *52*, 121–128.
(19) Yanisch-Perron, C.; Vieira, J.; Messing, J. *Gene* **1985**, *33*, 103–119.
(20) Kunkel, T. A.; Roberts, J. D.; Zakour, R. A. *Methods Enzymol.* **1987**, *154*, 367–82.
(21) Sanger, F.; Nicklen, S.; Coulson, A. R. *Biotechnology* **1992**, *24*, 104–108.

Steady-State Kinetics. Catalase activity was determined by the method of Rørth and Jensen,[22] and peroxidase activity was determined spectrophotometrically using ABTS (2,2′-azinobis-(3-ethlybenzothiazolinesulfonic acid)) ($\varepsilon = 36{,}800\ M^{-1}\ cm^{-1}$) and *o*-dianisidine ($\varepsilon_{460} = 11{,}300\ M^{-1}\ cm^{-1}$) as previously described.[13]

EPR Sample Preparation. The reaction of resting (ferric) enzymes with peroxyacetic acid resulted from mixing manually 40 uL of BpKatG (in 50 mM TRIS/maleate buffer, pH 6.4) with an equal volume of 10-fold excess buffered peroxyacetic acid (PAA) solution (pH 5.0) directly in the 4-mm EPR tubes kept at 0 °C. The reaction was stopped by rapid immersion of the EPR tube in liquid nitrogen after 10 s. The initial enzyme concentration used was 1 mM for the high-field/high-frequency (285 GHz) EPR experiments and 0.5 mM for the conventional (9 GHz) measurements. The excess of PAA and the mixing time used in these experiments were those providing the highest yield of the radical signals. No detectable differences in the relative contribution of the tyrosyl and tryptophanyl radical signals to the high-field EPR spectrum were observed for the wild-type enzyme in samples prepared with 5 or 20 s mixing times. Using lower excess of PAA (5-fold excess) resulted in the formation of the same EPR signal except for a lower yield, which scaled inversely with the conversion of the ferric iron signal. When mixing BpKatG with PAA at room temperature (20 °C) the same EPR spectrum was observed except for a lower yield of radical species. For the reaction with *tert*-butyl hydroperoxide (tBHP), the enzyme was mixed with 50-fold excess (pH 6.4) at 20 °C for 2 s. It is of note that the intensity of the EPR radical signal was $^1/_{10}$ of the intensity when using 10-fold excess tBHP and directly scaled with the lower conversion of the ferric signal of the resting enzyme. The same radical yield was obtained with 50-fold and 100-fold excess tBHP. Spin quantification of the different radical species in BpKatG was done using the signal of the exchange-coupled Trp radical from cytochrome *c* peroxidase[23] (at 4 K) and a bovine catalase tyrosyl radical[24] at 50 K (for the non-exchange-coupled $Trp^{\bullet}$ and $Tyr^{\bullet}$ species). The choice of references for spin quantification was done by considering radicals with comparable relaxation properties (related to radical-metal interaction) as well as line shapes.

Multifrequency EPR Spectroscopy. Conventional 9-GHz EPR measurements were performed using a Bruker ER 300 spectrometer with a standard TE_{102} cavity equipped with a liquid helium cryostat (Oxford Instruments) and a microwave frequency counter (Hewlett-Packard 5350B). The home-built high-field EPR spectrometer (95−285 GHz) has been described elsewhere.[25] The absolute error in *g*-values was 1×10^{-4}. The relative error in *g*-values between any two points of a given spectrum was 5×10^{-5}.

Results

Multifrequency EPR spectroscopy combined with site-directed mutagenesis (single, double, and triple variants) was applied to identify the protein-based radicals formed in *B. pseudomallei* KatG and also to assess their specific roles in the peroxidase-like reaction of the enzyme. Figure 1 summarizes our findings: Trp330, Trp139, and Trp153 (labeled in green) are the sites of [Fe(IV)=O $Trp^{\bullet}$] intermediates; Trp94 and Trp95 (labeled in blue) together with the extended H-bonding network of the heme distal side (red dotted line) constitute the pathway allowing the intramolecular electron transfer between Trp153 and the heme; Trp111 (labeled in blue) is required for the formation of the radical on Trp139, thus suggested as short-lived species in the superexchanged-coupled pathway to the heme cofactor. The experimental evidence for these assignments is described in the following sections.

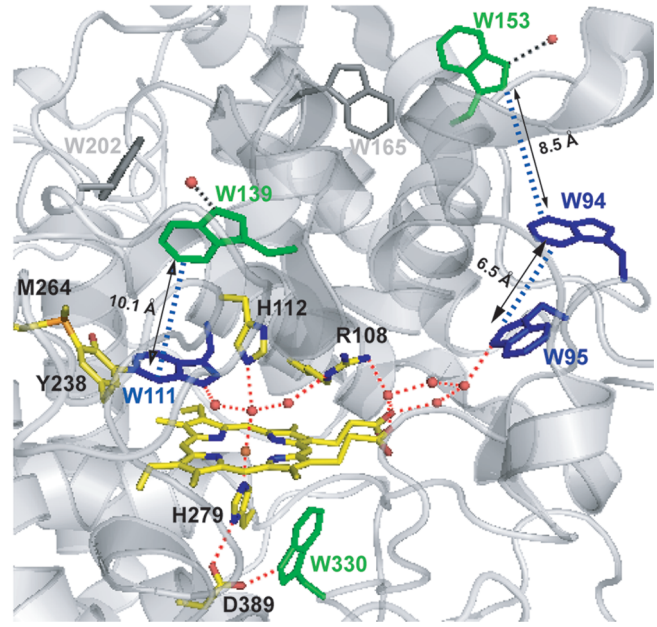

Figure 1. Crystallographic structure of the N-terminal domain of *B. pseudomallei* KatG (accession code 1MWV) showing the environment of the heme cofactor. Trp330, Trp139, and Trp153 (in green) are the radical sites identified by the EPR spectroscopy characterization. Trp95, Trp94, and Trp111 (in blue) are the specific residues shown to be involved in the long-range electron transfer pathways (blue dotted lines) between each radical site (Trp153 and Trp139) and the heme. Examples of the several other Trp positions that were also mutated and were shown to play no role as sites for radical formation or in electron transport pathways are shown in gray.

The Radical Intermediates in *B. pseudomallei* KatG Characterized by Multifrequency EPR Spectroscopy. BpKatG has been shown to efficiently disproportionate hydrogen peroxide,[26] necessitating the use of organic peroxides for a better characterization of the intermediates formed in the peroxidase cycle. Figure 2 shows the 9 GHz EPR spectrum, recorded at 4 K, of the enzyme upon reaction with 10-fold excess of PAA (top, black trace) and 50-fold excess tBHP (middle, gray trace). The EPR spectrum resulting from the reaction with 3-chlorobenzoic acid was identical to that of the PAA. The observed EPR signal centered at $g \approx 2$, with overall width of 400 G is indicative of an organic radical in magnetic interaction with the heme iron. The temperature dependence of this broad signal is the same as that reported for MtKatG[13] and agrees well with the expected behavior of an exchange-coupled radical species[27] as previously observed for the Trp radical in cytochrome *c* peroxidase.[14] Both Trp330 and Trp111 (see Figure 1), being fairly close and in indirect H-bonding interaction with the heme iron,[4] were good candidates for a radical with such magnetic properties. The location of Trp330 on the heme proximal side and in H-bonding distance to Asp389 (see Figure 1) is similar to that of the Trp radical site in cytochrome *c* peroxidase. In the latter, the removal of the H-bond donated by the aspartate

(22) Rorth, M.; Jensen, P. K. *Biochim. Biophys. Acta* **1967**, *139*, 171–173.
(23) Ivancich, A.; Dorlet, P.; Goodin, D. B.; Un, S. *J. Am. Chem. Soc.* **2001**, *123*, 5050–5058.
(24) Ivancich, A.; Jouve, H. M.; Gaillard, J. *J. Am. Chem. Soc.* **1996**, *118*, 12852–12853.
(25) Un, S.; Dorlet, P.; Rutherford, A. W. *Appl. Magn. Reson.* **2001**, *21*, 341–361.
(26) Singh, R.; Wiseman, B.; Deemagarn, T.; Jha, V.; Switala, J.; Loewen, P. C. *Arch. Biochem. Biophys.* **2008**, *471*, 207–214.
(27) Colvin, J. T.; Rutter, R.; Stapleton, H. J.; Hager, L. P. *Biophys. J.* **1983**, *41*, 105–108.

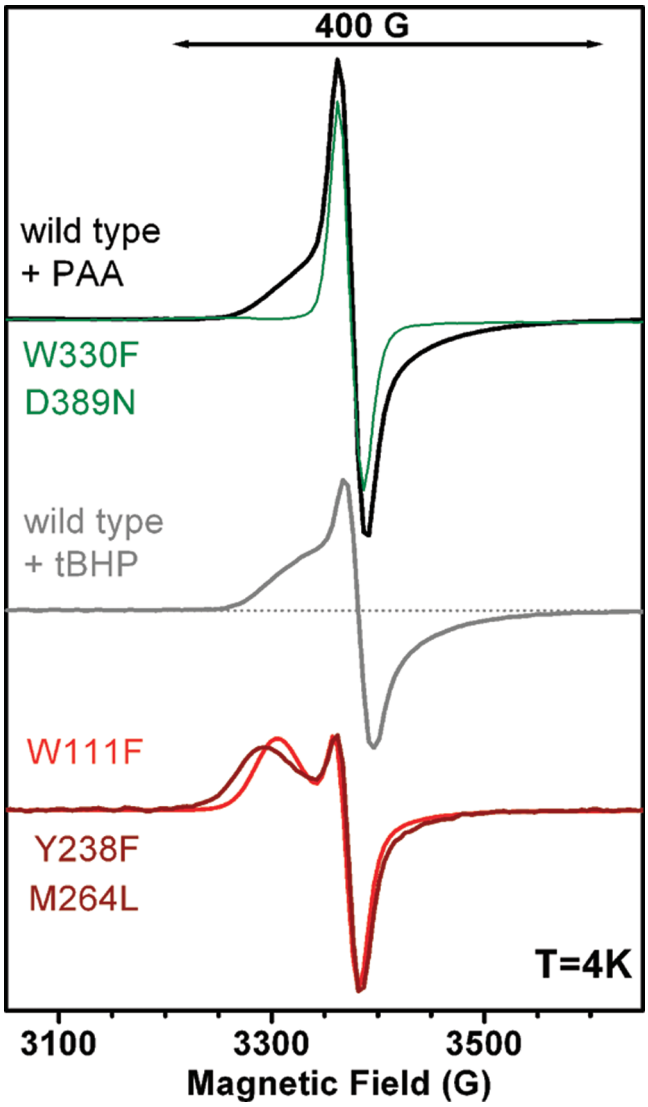

Figure 2. The 9-GHz EPR spectra, recorded at 4 K, of the radical intermediate(s) formed in wild-type (black trace) *B. pseudomallei* KatG and selected variants of the heme distal (red and dark red traces) and proximal (green traces) sides upon reaction with peroxyacetic acid. The spectrum obtained upon reaction of the wild-type enzyme with *tert*-butyl hydroperoxide is also shown (gray trace). Spectra were recorded at 4 K, 3 G modulation frequency, 1 mW microwave power, 100 kHz modulation frequency.

resulted in the absence of the exchanged-coupled radical EPR spectrum.[28,29] Trp111, on the heme distal side and also in indirect H-bonding interaction to the iron via a structural water molecule (see Figure 1) is part of an unusual adduct formed by the covalent linkage of Trp111, Tyr238, and Met264.[30] To investigate the role of these residues, we constructed and characterized the W330F, D389N, W111F, Y238F, and M264L variants of BpKatG. The 400 G-wide EPR signal was detected in all variants except W330F and D389N, for which only a clearly narrower radical signal was observed (Figure 2, green trace). These results are consistent

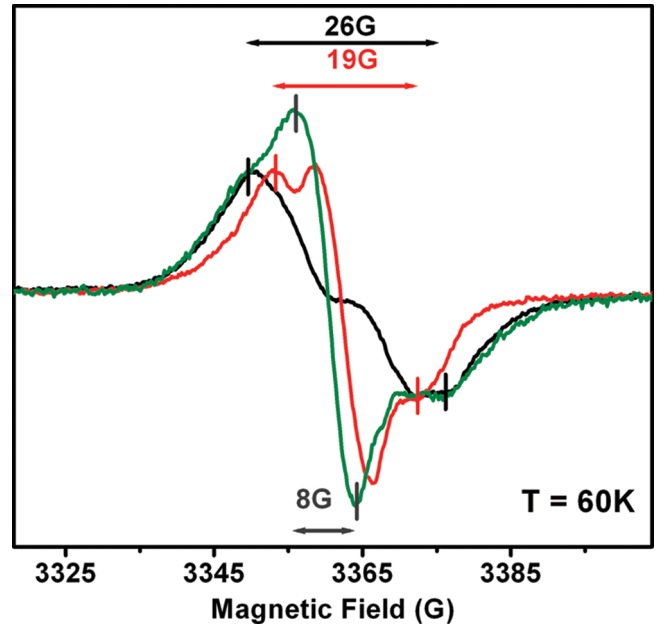

Figure 3. The 9-GHz EPR spectra, recorded at 60 K, of the protein-based radical species formed in wild-type *B. pseudomallei* KatG (black trace) upon reaction with peroxyacetic acid. Samples containing perdeuterated-Trp (red trace) or perdeuterated-Tyr (green trace) show line width and peak-to-trough differences consistent with selective perdeuteration of the $Trp^{\bullet}$ or $Tyr^{\bullet}$ species in each case. Spectra were recorded in nonsaturating conditions: 60K, 0.5 G modulation frequency, 0.08 mW microwave power, 100 kHz modulation frequency.

with Trp330 being the site of the exchange-coupled radical, stabilized by the H-bond to Asp389 as in MtKatG[13] and cytochrome *c* peroxidase.[14] The small difference in the line shape of the 400 G-wide radical spectra of the W111F, Y238F, and M264L variants (Figure 2, red and dark red traces) as compared to that of the wild-type (Figure 2, gray trace) can be rationalized by the direct (W111F) or indirect (Y238F and M264L) modifications on the hydrogen-bonding network of the heme distal side[6] induced by these mutations.

The contribution of a narrower signal to the central region of the 400G-wide EPR spectrum of the [Fe(IV)=O $Trp330^{\bullet+}$] species was evident when using PAA for the enzyme reaction (compare gray and black traces in Figure 2). Only this narrower signal, centered at $g \approx 2$ was detected for the W330F and D389N variants (Figure 2, green trace). The 9 GHz-EPR spectrum of the narrow radical recorded at 60 K was consistent with an isolated organic radical, effective isotropic *g*-value of 2.004 and peak-to-trough width of 26 G (Figure 3, black trace). The radical yields were estimated to be 0.5 spins/heme for the [Fe(IV)=O $Trp_{330}^{\bullet+}$] and 0.4 spins/heme for the narrow species. In order to unequivocally identify the chemical nature of the isolated radical we combined selective perdeuteration of Tyr and Trp residues with multifrequency EPR spectroscopy, as we have previously done in the case of MtKatG.[13] The 9-GHz EPR spectra of the perdeuterated samples recorded at 60 K (Figure 3) showed the expected changes due to the perdeuteration of the $Trp^{\bullet}$ or $Tyr^{\bullet}$ sites, as we have previously shown for the *Synechocystis* and *M. tuberculosis* KatGs.[12,13] Specifically, when using the perdeuterated-Trp sample, the narrower spectrum with a peak-to-trough width of 19 G (Figure 3, red trace) was entirely consistent with the expected predominant $Tyr^{\bullet}$ signal upon perdeuteration of the $Trp^{\bullet}$ species. Conversely, the perdeuter-

(28) Fishel, L. A.; Farnum, M. F.; Mauro, J. M.; Miller, M. A.; Kraut, J.; Liu, Y.; Ling Tan, X.; Scholes, C. P. *Biochemistry* **1991**, *30*, 1986–1996.
(29) Goodin, D. B.; McRee, D. E. *Biochemistry* **1993**, *32*, 3313–3324.
(30) Donald, L. J.; Krokhin, O. V.; Duckworth, H. W.; Wiseman, B.; Deemagarn, T.; Singh, R.; Switala, J.; Carpena, X.; Fita, I.; Loewen, P. C. *J. Biol. Chem.* **2003**, *278*, 35687–35692.
(31) Un, S. *Magn. Reson. Chem.* **2005**, *43*, S229–S239.

ated-Tyr sample (Figure 3, green trace) showed a spectrum with the same overall width and peak-to-trough (26 G) as the unlabeled sample and consistent with the predominant Trp$^{\bullet}$ signal. The much narrower signals (peak-to-trough of 8 G) of the perdeuterated-Trp$^{\bullet}$ and perdeuterated-Tyr$^{\bullet}$ species contributed to the central part of the nondeuterated species in each case. Such a narrowing of the EPR spectrum of the perdeuterated species is due to the difference in hyperfine couplings of protons and deuterium. The change in the unresolved Gaussian line width (ΔH) of the radical EPR spectrum in the deuterium-labeled samples as compared to the fully protonated spectrum is given by $\Delta H(^1\mathrm{H}) = [\gamma(^1\mathrm{H})/\gamma(^2\mathrm{H})]\ \sqrt{3}/8\ \Delta H(^2\mathrm{H})$, where γ denotes the gyromagnetic ratio of protons and deuteriums.

High-frequency EPR (HF-EPR) spectroscopy was applied to obtain the complementary information on the **g**-tensor of the (isolated) protein-based radicals by means of the enhanced resolution of the *g*-anisotropy at higher magnetic fields (see ref 25 and references therein). The 285-GHz EPR spectrum of the wild-type enzyme upon reaction with PAA and recorded at 10 K (Figure 4, panel A) clearly showed the contribution of two distinct protein-based radical species. The predominant signal could be simulated with *g*-values of 2.0036(3), 2.0027(6). and 2.0022(0) for g_x, g_y, and g_z respectively (Figure 3A, *inset*). The *g*-anisotropy, $\Delta g = |g_x - g_z| = 0.0014$, of this predominant signal in the HF-EPR spectrum is consistent with that expected for a tryptophanyl radical (see ref 31 and references therein). The observed *g*-values of the other signal contributing to the spectrum of 2.0064(4), 2.0040(5), and 2.0020(8) for g_x, g_x, and g_z respectively (see Figure 4A) agreed well with the intrinsic *g*-values expected for a tyrosyl radical (see ref 31 and references therein).

In the case of the W330F and W111F variants, the 285-GHz EPR spectra were also consistent with the formation of the (isolated) Trp and Tyr radicals (Figure 4A, green and red traces), in agreement with the deuteration studies on the same samples (see Figure S1 in Supporting Information). Yet, a remarkably lower intensity of the Trp$^{\bullet}$ signal was observed, in particular for W111F (Figure 4A, red trace) and was consistent with the clearly narrower EPR spectra recorded at 9-GHz on the same samples (Figure 4B, red trace). Trp330 and Trp111 are rather close to and involved in H-bonding interactions with the heme iron (see Figure 1). Hence, they can be ruled out as candidates for the noncoupled Trp$^{\bullet}$ site. Hence, the effect of these mutations on the yield of the (isolated) Trp$^{\bullet}$ species suggested a nontrivial relationship between these residues and the radical site. Taking into account the possible explanations for this experimental observation we designed, constructed, and characterized a set of Trp variants in order to identify the radical site(s).

Selected Mutations of Trp Residues for the Identification of the Radical Intermediate(S). The crystal structure of BpKatG shows that the majority of the Trp residues (17 out of the total number of 23 tryptophans) are in the N-terminal domain that binds the heme cofactor. Most of these tryptophans are located on the heme distal-side, organized in a sort of belt-shaped motif. An additional criterion used to narrow down the possible candidates for the Trp radical site was the presence of an H-bond partner, indicated by the *g*-values of the HF-EPR spectrum. Accordingly, Trp309, Trp208, Trp202, Trp139, Trp195, Trp165, and Trp153, all being in H-bonding distance to a water molecule, were chosen as candidates for the radical site. In addition, considering our previous findings in SynKatG[13] of a single Trp$^{\bullet}$ intermediate (Trp106 in SynKatG numbering) requiring the integrity of the extended H-bonding network for its stabilization, we constructed the equivalent variants in BpKatG. Accordingly, W95F (equivalent to the radical site in SynKatG), W94F (the adjacent residue to Trp95), and W111H (complementary information to the W111F on the effect of the H-bonding network[16]) variants were also characterized. The 9-GHz EPR spectra of the radical signals obtained for the Trp variants are shown in Figure 5. The intensities of the radical signals of

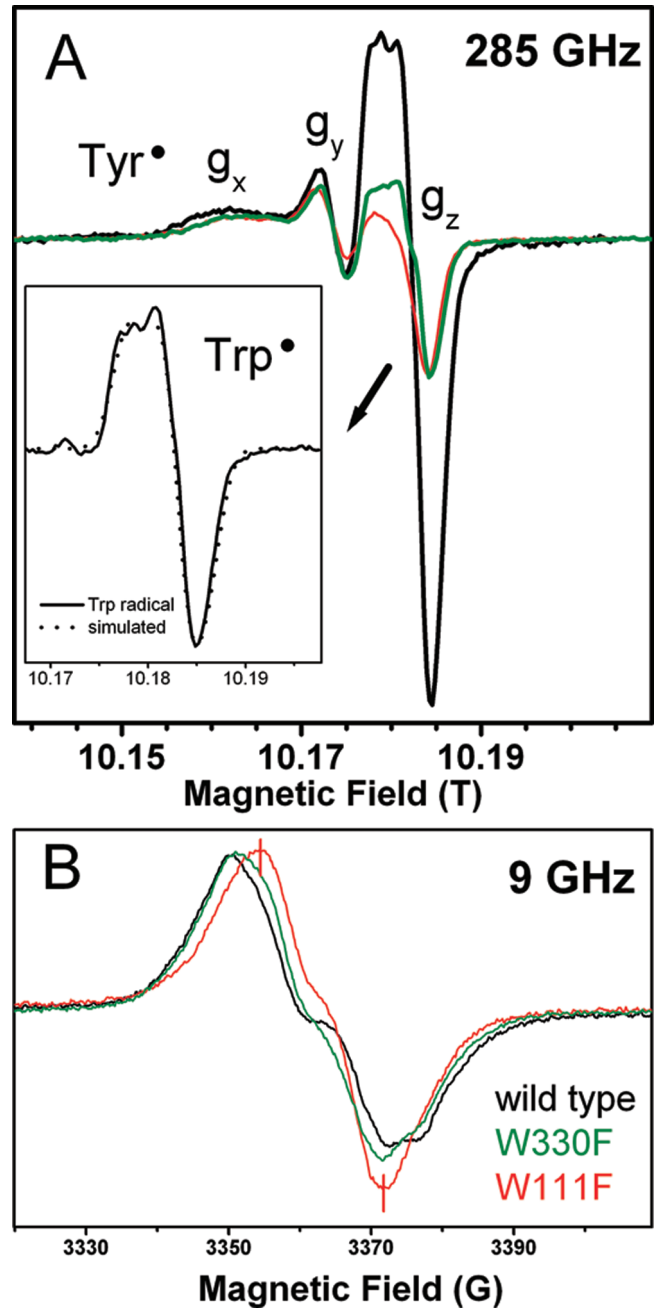

Figure 4. (Panel A) The high-field/high-frequency (10 T/285 GHz) EPR spectra of the protein-based radicals in wild-type (black trace) *B. pseudomallei* KatG and the W330F (green trace) and W111F (red trace) variants. Spectra were recorded at 10 K, using a frequency modulation of 30 kHz and a field modulation of 10 G. Each spectrum was recorded at slightly different microwave frequencies; for comparison, all the spectra are aligned to a nominal field. The inset shows the HF-EPR spectrum of the Trp$^{\bullet}$-only signal obtained by arithmetic subtraction of a Tyr$^{\bullet}$-only spectrum of the W191F variant of cytochrome *c* peroxidase.[23] (Panel B) The 9 GHz EPR spectra of same samples used for the high-field EPR experiments (Panel A). Experimental conditions as in Figure 2.

(32) Sharp, K.; Mewies, M.; Moody, P. C. E.; Raven, E. L. *Nat. Struct. Biol.* **2003**, *10*, 303–307.

variants W153F and W139F were both lower than wild type (Figure 5A). No such effect was caused by the mutation of other tryptophans in their close proximity (see Trp165 and Trp202 in gray, Figure 1). The W94F variant (but not the W95F) exhibited a distinct behavior with a radical yield 1.5 times higher than that of the wild-type enzyme (Figure 5B, blue trace). Replacing the distal Trp111 by histidine (W111H) also caused the same higher yield of the radical species (by a factor of 1.4; Figure 5C), while very little or no Trp was formed in the phenylalanine mutant W111F (Figure 5C, red trace).

A working hypothesis for a functional model consistent with these experimental results was the following: radicals forming on Trp153 and Trp139 were both contributing to the EPR signal of the wild-type enzyme. Therefore, each point mutation (W139F and W153F) impaired the formation of only one radical, giving rise to the lower radical yield for each variant. Trp153 is not close enough to the heme (see distances in Figure 1) for a single-step electron tunneling event to occur.[10,11] A most obvious electron pathway between Trp153 and the heme (blue dotted line in Figure 1) involves Trp94, the adjacent Trp95, and the water matrix, all part of the extended H-bonding network[14] of the heme distal side (see red dotted line in Figure 1). In the case of the radical formed at Trp139, the distal Trp111 could play a role in facilitating electron transport to the heme (see blue dotted line in Figure 1). Accordingly, Trp111 would have a functional role as electron relay in the formation of the radical at Trp139, as well as a more passive, and yet crucial, role in maintaining the integrity of the extended H-bonding network related to the formation of the radical at Trp153. This dual role of Trp111 would account for the experimental observations on the W111F and W111H variants. The question remains whether in the absence of the Trp153 radical site or the electron transfer pathway related to it, a longer-lived radical would be stabilized on Trp95, the site in SynKatG.

Figure 5D shows the protein-based EPR spectra of the radicals formed by the reaction with PAA of three triple variants that were specifically designed to test our working hypothesis about electron transfer pathways and radical sites (see above). The W153F+W139F+W330F variant was designed to remove the three radical sites (see Figure 1, residues labeled in green). The W94F+W139F+W330F variant was designed to impede formation of $Trp153^{\bullet}$ by removing one of the putative tryptophans in the pathway (Trp94, see Figure 1) and to remove the two other Trp radical sites (Trp330 and Trp139). The W95F+W139F+W330F variant was designed as a control to the W153F+W139F+W330F variant for testing if Trp95 could become a more stable radical when $Trp330^{\bullet}$ and $Trp139^{\bullet}$ cannot form (hence mimic the situation in SynKatG). The EPR spectra of the W153F+W139F+W330F (Figure 5D, dark green trace) and W94F+W139F+W330F (Figure 5D, light-green traces) variants both showed a $Trp^{\bullet}$ signal of higher intensity than wild type (Figure 5D, black trace). Progressive microwave power saturation studies on these radicals indicated that the saturation conditions of these signals were different from those of the wild-type enzyme. The result is consistent with a radical site with different magnetic interaction to the heme iron in these variants as compared to that of the radicals in the wild-type enzyme. The W95F+W139F+W330F variant showed a clearly narrower radical with peak-to-trough of 19 G (Figure 5D, red trace), consistent with a $Tyr^{\bullet}$-only spectrum as in the case of the W111F variant (Figure 5C, red trace). Taken together, these results support our working hypothesis of a longer-lived Trp95 radical stabilized in the absence of the primary radical sites (Trp330, Trp139, and Trp153).

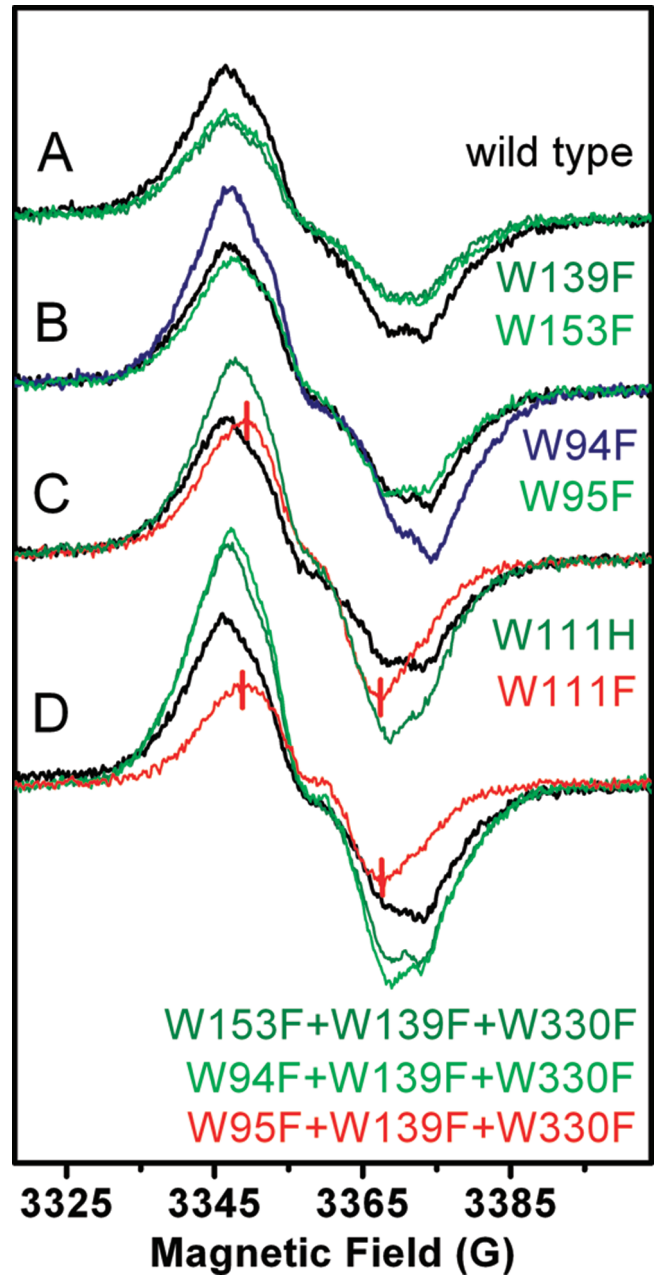

Figure 5. Comparisons of the 9-GHz EPR spectra, recorded at 50 K, of the single and triple mutations of selected tryptophans. The variants were designed and constructed in order to identify the $Trp^{\bullet}$ sites and the putative electron transfer pathways (see Results section). Experimental conditions as in Figure 1.

Discussion

Our previous EPR investigation of the radical intermediates of two other catalase-peroxidases[12,13] indicated that the sites for the relatively long-lived Trp radical intermediates can be different, an equivalent situation to the well-documented cases in monofunctional peroxidases. Specifically, in SynKatG the [Fe(IV)=O $Por^{\bullet+}$] and a subsequent [Fe(IV)=O $Trp^{\bullet}$] species with the radical site on Trp106 (equivalent to Trp95 in Figure 1) were detected. The situation in SynKatG is then comparable to that of lignin peroxidase,[14] but in the latter the lifetime of the intermediates is reversed (longer-lived [Fe(IV)=O $Por^{\bullet+}$]

species). MtKatG showed a very similar behavior to cytochrome c peroxidase,[15] with the formation of an exchange-coupled radical species [Fe(IV)=O $Trp^{\bullet+}$] on the proximal Trp321 (equivalent to Trp330 in Figure 1) subsequent to the short-lived [Fe(IV)=O $Por^{\bullet+}$] species. Another $Trp^{\bullet}$ signal was identified in MtKatG, but mutation of the Trp site identified in SynKatG (Trp95 in Figure 1) did not result in the suppression of the EPR $Trp^{\bullet}$ signal. This $Trp^{\bullet}$ species was involved in the peroxidase reaction of MtKatG with isoniazid.[13] We then considered that understanding the apparent differences of radical location in two such similar enzymes was of high interest.

In this work, the thorough characterization of *B. pseudomallei* KatG allowed us to obtain a complete picture of the specific sites for Trp radicals as alternative intermediates to the [Fe(IV)=O $Por^{\bullet+}$] species in catalase-peroxidases. It also provided a frame to explain the cases of peroxidases, such as CcP and lignin peroxidase in which tryptophanyl radicals are also reactive intermediates but have been considered as exceptions within monofunctional peroxidases. Trp330, Trp139 and Trp153 were identified as the three distinct sites for the radical formation in BpKatG (see Figure 1, residues in green). Consequently, the proximal Trp330 appears to be a conserved radical site in KatGs and monofunctional CcP. The exception of the cyanobacterial KatGs is possibly explained by a different equilibrium between radical intermediates, supported by the observed longer-lived [Fe(IV)=O $Por^{\bullet+}$] species in SynKatG.[12] All three tryptophans are involved in a H-bond interaction with either an Asp residue (for Trp330) or a water molecule (Trp139 and Trp153) as shown in Figure 1. Moreover, the presence of a methionine residue close to Trp330 (S_{Met} to N_{indole} distance of 4.7 Å) and Trp139 (S_{Met} to N_{indole} distance of 5.1 Å) could contribute to stabilization of the $Trp^{\bullet}$ intermediates, as previously proposed for the Trp radical in CcP.[33] Trp153 is close to the enzyme surface (see Figure 1) and could act as oxidation site for yet to be identified bulky substrates. Trp330 and Trp139 are more deeply buried into the protein (see Figure 1) but they are close to access channels identified in the crystallographic structure.[4] Work is in progress in order to correlate EPR studies on the reactivity of these two radicals with putative substrate binding sites of isoniazide.

The other important aspect revealed in this work is the role of specific tryptophans in facilitating electron transfer between Trp153 or Trp139 and the heme cofactor. Specifically, combination of single and triple mutants indicated that Trp 94, Trp95 (equivalent to the unique radical site, Trp106, in SynKatG[16]) and the water matrix constitute a most likely electron transport pathway between Trp153 and the heme (Figure 1, dotted lines in red and blue). The closest distance measured between the macrocycle edge of the heme[34] and Trp153 is about 23 Å. It has been shown that distances up to 14 Å allow biologically relevant single-step electron tunneling through the protein matrix.[10] For longer distances, the presence of one or more Trp residues is required to enhance the electron transfer rates.[11] Then, Trp94 and Trp95 are positioned at distances of less than 10 Å (see Figure 1) that allow efficient electron transfer between Trp153 and the heme edge. In the case of Trp139, the minimum distance between the N_{indole} and the heme edge (13.8 Å) may allow single-step electron tunneling to the heme. However, the EPR characterization of the W111F and W111H variants indicated the need of Trp111 for the radical formation on Trp139. This observation implies that a transient radical on Trp111 is involved in superexchange-coupled pathways (see blue dotted line in Figure 1). Also, Trp111 is part of the distal side extended H-bonding network (red dotted line in Figure 1) involved in the formation of Trp153 (see above). Hence, replacing Trp111 by Phe impeded the formation of both Trp139 and Trp153 radicals, while its replacement with His (that restores the extended H-bonding network) only impeded the Trp139 formation. Therefore, our findings show that the extended H-bonding network and the Trp-Tyr-Met adduct (unique structural features of the heme distal side in KatGs) are required for the formation of the protein-based radical intermediates in the peroxidase reaction as well as for the catalase-like reaction of KatGs. Moreover, it is shown that BpKatG constitute a particularly interesting enzyme to investigate further biological electron transfer.

Our findings also indicate that the ferryl intermediate with the second oxidizing equivalent delocalized on the proximal Trp or another Trp site away from the heme pocket, forming at the expense of a short-lived [Fe(IV)=O $Por^{\bullet+}$] species, may be considered as an early functional feature for differentiation of the peroxidase-like and the catalase-like reactions of KatGs. In this way, the occurrence of alternative oxidizing sites for the one-electron oxidation of substrates (distant from the heme microenvironment) would compensate for the restrained access channel and fine-tuned heme pocket, required for the catalase-like reaction in KatGs. Cytochrome *c* and lignin peroxidases (as well as lactoperoxidase) would have partially conserved this functional feature (protein-based radicals) as shown by the formation of alternative oxidizing sites. In contrast, most of the plant peroxidases developed a specific substrate interaction site close to the δ-meso edge of the heme for an efficient substrate oxidation using the more persistent [Fe(IV)=O $Por^{\bullet+}$] intermediate. Also, the fact that the binding site of ascorbate[32] in ascorbate peroxidase is coincident with the extended H-bonding network in KatGs (see red dotted line in Figure 1) and the Trp radical site of SynKatG[16] may reflect conservation of an earlier functional feature. In conclusion, identification of the intermediates formed in the peroxidase-like reaction of BpKatG allowed us to elaborate a comprehensive picture of the role of specific Trp residues that takes into account not only the apparent differences in sites for the $Trp^{\bullet}$ intermediates in other catalase-peroxidases but also the similar cases observed in monofunctional peroxidases.

Acknowledgment. This work was supported by the French CNRS and CEA Saclay (to A.I.), a Ph.D. Fellowship (CFR contract from CEA Saclay to J.C.) and grants from the Natural Sciences and Engineering Research Council of Canada (to P.C.L.) and the Canadian Research Chair Program (to P.C.L.). We thank Sun Un (CEA Saclay) for insights and discussions on HF-EPR spectroscopy and Harry Gray (Caltech) for stimulating discussions on the role of tryptophans in electron transfer.

Supporting Information Available: The 9-GHz EPR spectra, recorded at 60 K, of the protein-based radical species formed in W330F and W111F variants of *B. pseudomallei* KatG showing the effect of selective deuteration of Trp and Tyr residues. This material is available free of charge via the Internet at http://pubs.acs.org.

JA901402V

(33) Jensen, G. M.; Bunte, S. W.; Warshel, A.; Goodin, D. B. *J. Phys. Chem. B* **1998**, *102*, 8221–8228.
(34) Moser, C. C.; Chobot, S. E.; Page, C. C.; Dutton, P. L. *Biochim. Biophys. Acta* **2008**, *1777*, 1032–1037.